

ISSN: 0095-8972 (Print) 1029-0389 (Online) Journal homepage: <http://www.tandfonline.com/loi/gcoo20>


Synthesis, characterization, DNA interaction, and in vitro cytotoxicity activities of two ruthenium(II) complexes with disubstituted 2,2'-dipyridyl ligands bearing ammonium groups

Jing Sun, Wen-Xiu Chen, Xing-Dong Song, Xuan-Hao Zhao, Ai-Qing Ma & Jia-Xi Chen


To cite this article: Jing Sun, Wen-Xiu Chen, Xing-Dong Song, Xuan-Hao Zhao, Ai-Qing Ma & Jia-Xi Chen (2015) Synthesis, characterization, DNA interaction, and in vitro cytotoxicity activities of two ruthenium(II) complexes with disubstituted 2,2'-dipyridyl ligands bearing ammonium groups, Journal of Coordination Chemistry, 68:2, 308-320, DOI: [10.1080/00958972.2014.977270](https://doi.org/10.1080/00958972.2014.977270)

To link to this article: <http://dx.doi.org/10.1080/00958972.2014.977270>

 View supplementary material 

 Accepted author version posted online: 15 Oct 2014.
Published online: 10 Nov 2014.

 Submit your article to this journal 

 Article views: 83

 View related articles 

 View Crossmark data 

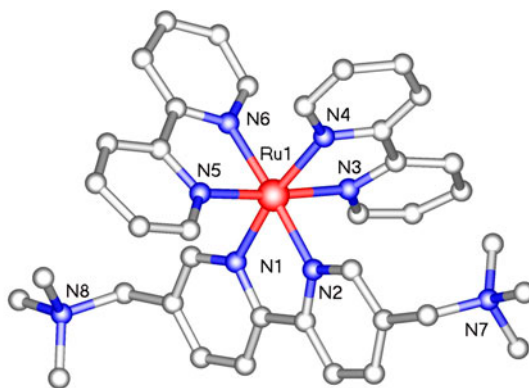
 Citing articles: 5 View citing articles 

Synthesis, characterization, DNA interaction, and *in vitro* cytotoxicity activities of two ruthenium(II) complexes with disubstituted 2,2'-dipyridyl ligands bearing ammonium groups

JING SUN*, WEN-XIU CHEN, XING-DONG SONG, XUAN-HAO ZHAO,
AI-QING MA and JIA-XI CHEN*

School of Pharmacy, Guangdong Medical College, Dongguan, China

(Received 18 June 2014; accepted 25 September 2014)



The DNA binding, cleavage, and cytotoxic properties of two new Ru(II) complexes $[\text{Ru}(\text{bpy})_2\text{L}](\text{PF}_6)_4$ (L: $\text{L}^1 = (5,5'-(n\text{-Me})_3\text{NCH}_2)_2\text{-bpy}^{2+}$; $\text{L}^2 = (5,5'-(n\text{-Et})_3\text{NCH}_2)_2\text{-bpy}^{2+}$) have been investigated. The results show that both Ru(II) complexes bind to DNA through an electrostatic binding mode. The binding affinity constant can reach 10^4 M^{-1} and **1** has a higher binding affinity than **2**. Equilibrium dialysis experiments revealed that the complexes are candidates for enantioselective binding to CT-DNA. Moreover, further analysis of the ruthenium complexes revealed that **1** has a higher and more efficient DNA cleavage activity than **2**. *In vitro* cytotoxicity studies of both complexes showed that they exhibited moderate antitumor activity against HeLa, A549, and CNE-2 cancer cells. In addition, **2** displayed higher *in vitro* cytotoxicity than **1**.

Keywords: Synthesis; Ru(II) complex; DNA-binding; Photocleavage; Cytotoxicity

*Corresponding authors. Email: sunjing03@foxmail.com (J. Sun); zppcc@qq.com (J.-X. Chen)

1. Introduction

Ruthenium complexes have been synthesized and explored for potential use as DNA structure probes, DNA cleavage mediators, DNA footprinting, and chemotherapeutic agents. The burgeoning number of ruthenium complexes is due to the ease at which rigid Ru(II) complexes that span at all 3-D can be constructed. In addition, ruthenium complexes exhibit rich photophysical and photochemical properties [1–6]. Previous studies suggested that Ru(II) complexes can bind to DNA by non-covalent interactions such as electrostatic binding, groove binding, intercalative binding, and partial intercalative binding [2]. Previous experimental results have shown that subtle changes in the molecular structures of Ru(II) complexes might bring about substantial effects on the binding modes, sites, and affinities. The ability to induce the formation of different Ru(II) complexes provided the chance to further explore and acquire information on conformation and site-specific DNA probes. Great efforts have been devoted to modify the polypyridine ligands, resulting in some interesting differences in the spatial configurations of Ru(II) polypyridine complexes which in turn resulted in some important differences in the DNA binding behavior of these complexes. Among them, many Ru(II) complexes that can be formed, polypyridine ligands play an important role in determining and improving their light emitting and electron transfer performances [7–10]. In other complexes [11–15], different polypyridine ligands exhibit higher *in vitro* cytotoxicity against different human cancer cells.

Molecules that interact with and further stabilize DNA have the following properties: (a) a π -delocalized system, (b) a partial positive charge in the center of the molecular scaffold, and (c) a positively charged substituent to interact with the grooves, loops, and the negatively charged phosphate backbone [16]. Determining how metal complexes bind DNA will not only pave the way to understand the fundamentals of these molecular interactions, but also potentially provide new therapeutic applications. The development of synthetic and sequence-selective DNA binding, DNA cleavage agents, and new potential DNA-targeted antitumor drugs is essential to further advance molecular biology, medicine, and other related fields.

Herein, we report the syntheses, characterizations, DNA binding, cleavage, and cytotoxic abilities of two ruthenium(II) polypyridyl complexes containing quaternary ammonium 2,2'-dipyridyl derivatives. Complex **1** was structurally characterized by single-crystal X-ray crystallography.

2. Experimental

2.1. Materials and methods

CT-DNA was purchased from Sigma Company and pBR322 DNA from Sangon Biotechnology Company. 5,5'-Dimethyl-2,2'-dipyridyl was purchased from Aldrich Chemical Co. Buffer A (5.0 mM tris(hydroxymethyl)aminomethane tris-hydrochloride, 50 mM NaCl, pH 7.2) was used for viscosity, absorption titration, and dialysis experiments, buffer B (1.5 mM Na₂HPO₄, 0.5 mM NaH₂PO₄, 0.25 mM Na₂EDTA, pH 7.0) was used for thermal DNA denaturation experiments, and buffer C (50 mM Tris-HCl, 18 mM NaCl, pH 7.2) was used for DNA photocleavage experiments. CT-DNA dissolved in either buffer A or B gave a

ratio of UV absorbance of 1.8–1.9 : 1 at 260 and 280 nm, suggesting that the DNA was sufficiently free of protein [17]. The concentration of DNA was determined spectrophotometrically, assuming that the molar absorption was $6600 \text{ M}^{-1} \text{ cm}^{-1}$ (260 nm) [18]. All reagents and solvents were purchased commercially and used without further purification unless noted. Double distilled water was used to prepare buffer solutions.

2.2. Physical measurement

Elemental analyses (C, H, and N) were carried out with a Perkin Elmer 240C elemental analyzer. ^1H NMR spectra were recorded on a Varian Mercury-plus 300 NMR spectrometer with DMSO-d_6 as solvent and SiMe_4 as an internal standard at 300 MHz at room temperature. Electrospray ionization mass spectrometry (ESI-MS) was recorded on an LQC system (Finnigan MAT, USA) using CH_3CN as the mobile phase. UV and visible spectra were measured using a Perkin Elmer Lambda-850 spectrophotometer.

2.3. Preparation of ligands and complexes

$\text{L}^1\text{Br}_2 \cdot 2\text{H}_2\text{O}$ [19], $\text{L}^2\text{Br}_2 \cdot 4\text{H}_2\text{O}$ [20], and *cis*- $[\text{Ru}(\text{bpy})_2\text{Cl}_2] \cdot 2\text{H}_2\text{O}$ [21] were prepared and characterized according to the literature.

2.3.1. $[\text{Ru}(\text{bpy})_2(\text{L}^1)](\text{PF}_6)_4 \cdot \text{CH}_3\text{OH}$ (1). A mixture of *cis*- $[\text{Ru}(\text{bpy})_2\text{Cl}_2] \cdot 2\text{H}_2\text{O}$ (0.26 g, 0.5 mM), $\text{L}^1\text{Br}_2 \cdot 2\text{H}_2\text{O}$ (0.24 g, 0.5 mM), and ethylene glycol (20.0 cm^3) was heated at 130°C under the protection of argon for 6 h, during which the solution turned red. The solution was cooled to room temperature. After filtration, dropwise addition of saturated NH_4PF_6 resulted in a red-orange precipitate which was then filtered and recrystallized with $\text{CH}_3\text{CN}/\text{CH}_3\text{OH}$ (1 : 1, *v/v*), and red single crystals were obtained. Yield: 0.54 g (82.3%). Anal. Calcd for $\text{C}_{38}\text{H}_{44}\text{F}_{24}\text{N}_8\text{P}_4\text{Ru} \cdot \text{CH}_3\text{OH}$ (1, 1325.78): C, 35.33; H, 3.65; N, 8.45. Found: C, 35.50; H, 3.69; N, 8.47. ESI-MS: $m/z = 1148.9$ $[\text{M}-\text{PF}_6^-]^+$ (21), 502.0 $[\text{M}-\text{PF}_6^-]^{2+}$ (100), 286.4 $[\text{M}-3\text{PF}_6^-]^{3+}$ (65). ^1H NMR (DMSO-d_6): δ 9.02 (d, 2H); 8.79 (d, 4H); 8.32 (d, 2H); 8.16 (t, 4H); 7.88 (d, 2H); 7.75 (s, 2H); 7.65 (d, 2H); 7.49 (dd, 4H); 4.18 (s, 4H); 2.90 (s, 18H).

2.3.2. $[\text{Ru}(\text{bpy})_2(\text{L}^2)](\text{PF}_6)_4 \cdot 2\text{H}_2\text{O}$ (2). This complex was obtained using a procedure similar to that previously described for 1. $\text{L}^2\text{Br}_2 \cdot 4\text{H}_2\text{O}$ (0.30 g, 0.5 mM) was used instead of $\text{L}^1\text{Br}_2 \cdot 2\text{H}_2\text{O}$. The crude product was purified by column chromatography on alumina using acetonitrile as eluent. Yield: 0.57 g (80.6%). Anal. Calcd for $\text{C}_{44}\text{H}_{56}\text{F}_{24}\text{N}_8\text{P}_4\text{Ru} \cdot 2\text{H}_2\text{O}$ (2, 1413.93): C, 37.38; H, 4.28; N, 7.92. Found: C, 37.49; H, 4.21; N, 7.92. $m/z = 1233.0$ $[\text{M}-\text{PF}_6^-]^+$ (25), 544.1 $[\text{M}-\text{PF}_6^-]^{2+}$ (100), 314.5 $[\text{M}-3\text{PF}_6^-]^{3+}$ (38). ^1H NMR (DMSO-d_6): δ 9.90 (d, 2H); 8.83 (d, 4H); 8.27 (d, 2H); 8.17 (dd, 4H); 7.83 (d, 2H); 7.75 (s, 2H); 7.67 (d, 2H); 7.51 (dd, 4H); 4.45 (s, 4H); 3.04 (q, 12H), 1.10 (t, 18H).

2.4. X-ray crystallography

Single-crystal X-ray diffraction experiments were carried out with a Bruker Smart Apex CCD area detector at $153(2)$. The dimensions of crystals of the complex used for X-ray diffraction analysis was $0.18 \times 0.16 \times 0.04$ mm. Data collection was performed with $\text{Cu-K}\alpha$

Table 1. Crystallographic data of **1** [Ru(bpy)₂(5,5'-(Me₃NCH₂)₂-bpy)](PF₆)₄·CH₃OH.

Complex	[Ru(bpy) ₂ (5,5'-(Me ₃ NCH ₂) ₂ -bpy)](PF ₆) ₄ ·CH ₃ OH
Empirical formula	C ₃₉ H ₄₈ F ₂₄ N ₈ OP ₄ Ru
Formula weight	1321.77
Temperature (K)	150(2)
Wavelength (Å)	1.54178
Crystal system, space group	Monoclinic, <i>P21/c</i>
<i>a</i> (Å)	12.4949(3)
<i>b</i> (Å)	32.2746(8)
<i>c</i> (Å)	17.9132(6)
<i>α</i> (°)	90.00
<i>β</i> (°)	131.029(2)
<i>γ</i> (°)	90.00
Volume (Å ³)	5449.5(3)
<i>Z</i>	2
<i>D</i> _{Calcd} (g cm ⁻³)	1.611
<i>F</i> (0 0 0)	2648
Crystal size (mm)	0.18 × 0.16 × 0.04
<i>θ</i> Range for data collection	2.87 to 26.00
Limiting indices	-15 ≤ <i>h</i> ≤ 15, -37 ≤ <i>k</i> ≤ 39, -14 ≤ <i>l</i> ≤ 22
Reflections collected	22134
Independent reflections	10283 (<i>R</i> _{int} = 0.0413)
Goodness-of-fit on <i>F</i> ²	0.970
<i>R</i> ₁ / <i>wR</i> ₂ [<i>I</i> > 2σ(<i>I</i>)] ^a	0.0827/0.2457
<i>R</i> ₁ / <i>wR</i> ₂ (all data)	0.1222/0.2712
Largest diff. peak (e Å ⁻³)	1.912/-1.219

radiation ($k = 1.54178$ Å). Absorption corrections were applied using SADABS [22] and the structures were solved by direct methods. All non-hydrogen atoms were refined anisotropically by least-squares on F^2 using SHELXTL [23]. These were first refined isotropically and then anisotropically. The hydrogens of the ligands were placed in calculated positions with fixed isotropic thermal parameters and structure factor calculations were included in the final stage of full-matrix least-squares refinement. A summary of the crystal data is given in table 1.

2.5. DNA-binding experiments

Viscosity measurements were carried out using an Ubbelohde viscometer maintained at a constant temperature of 30.0 ± 0.1 °C in a thermostatic bath. DNA samples with an approximate average length of 200 base pairs were prepared by sonication in order to minimize the complexities arising from DNA flexibility [24]. Flow time was measured with a digital stopwatch. Each sample was measured three times and an average flow time was then calculated. The data are presented as $(\eta/\eta^0)^{1/3}$ versus binding ratio ($[\text{Ru}]/[\text{DNA}]$) [25], where η^0 was the viscosity of DNA in the presence of complex while η^0 was the viscosity of DNA alone.

The absorption titration of Ru(II) complexes in buffer A was performed using a fixed complex concentration to which increments of the DNA stock solution were added. The concentration of the $[\text{Ru}(\text{bpy})_2(\text{L})]^{4+}$ solution was 10 μM and the volume of complex was 3000 μL. Complex-DNA solutions were allowed to incubate for 5 min before the spectra were recorded. The titration processes were repeated several times until no change was observed in the spectra, which indicated that binding saturation was achieved. Changes in the Ru(II) complex concentration due to dilution at the end of each titration were negligible.

Thermal denaturation of DNA was carried out with a Perkin Elmer Lambda 850 spectrophotometer equipped with a Peltier temperature-control programmer (± 0.1 °C). The temperature of the solution was increased from 40 to 90 °C at a rate of 1 °C min⁻¹ and the absorbance at 260 nm was continuously monitored for solutions of DNA (100.0 μ M) in the absence and presence of the Ru(II) complex (10.0 μ M). The data were presented as $(A - A_f) / (A_0 - A_f)$ versus temperature, where A , A_f , and A_0 were the observed absorbances at temperature T , at 90 °C, and at 40 °C, respectively, at 260 nm.

Equilibrium dialysis was carried out in the dark and held at room temperature for 12 h with 5 mL of CT-DNA (1.0 mM) sealed in a dialysis bag and 10 mL of the Ru(II) polypyridine complexes (50 μ M) outside the bag. The bandwidth was 1 nm and the response time was 1 s. Spectral data were collected at 0.1 nm intervals with a scan speed of 300 nm min⁻¹ three times at each CD spectrum. DNA was thoroughly dialyzed prior to conducting the experiments. Ru(II) complexes were used as blanks for the equilibrium dialysis and CD studies. Ru(II) polypyridine complex blanks showed no detectable CD signal.

2.6. DNA photocleavage experiments

During the gel electrophoresis experiments, supercoiled pBR322 DNA (0.10 μ g) was treated with a Ru(II) complex in buffer C, and the solution was subsequently irradiated at room temperature with a UV lamp (365 nm, 10 W) for 60 min. The samples were analyzed by electrophoresis for 2 h at 80 V on 1.0% agarose gel in a TBE buffer (89 mM tris-borate acid, 2.0 mM EDTA, pH 8.3). The gel was stained with ethidium bromide (EB = 3,8-diamino-5-ethyl-6-phenylphenanthridinium bromide, 1.0 μ g mL⁻¹) and photographed with an Alpha Innotech IS-5500 fluorescence chemiluminescence and visible imaging system.

2.7. Cytotoxicity assays

Cells were placed in 96-well microassay culture plates (5×10^3 cells per well) and incubated overnight at 37 °C in a 5% CO₂ incubator. Test metal complexes were then added to the wells to achieve final concentrations. Control wells were prepared by addition of culture medium. Wells containing culture medium without cells were used as blanks. Twenty microliters of a stock MTT dye solution (5 mg mL⁻¹) was added to each well after 48 h incubation. DMSO (100 μ L) was added to solubilize the MTT (3-(4,5-dimethylthiazol-2-yl)-2,5-diphenyltetrazolium bromide) formazan after an additional incubation period of 4 h. The optical density of each well was then measured on a microplate spectrophotometer at 630 nm. IC₅₀ values of the target compounds were calculated using SPSS Statistics 17.0 and expressed as mean \pm SD of triplicate experiments. HeLa, A549, and CEN-2 human tumor cell lines were the subjects of this study.

3. Results and discussion

3.1. Description of the molecular structure

Figure 1 depicts the structure of **1**. Selected bond distances and angles are given in table 2. The complex contains a six-coordinate ruthenium chelated by two bpy and one dicationic L¹, four PF₆⁻ anions, and one CH₃OH. The coordination geometry about ruthenium is a

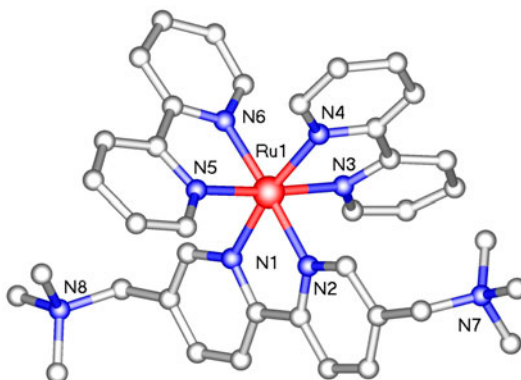


Figure 1. X-ray crystal structure of **1**. All hydrogens are omitted for clarity.

Table 2. Selected bond lengths (Å) and angles (°) for **1**.

Ru(1)–N(1)	2.067(5)	Ru(1)–N(2)	2.046(5)
Ru(1)–N(3)	2.054(5)	Ru(1)–N(4)	2.056(5)
Ru(1)–N(5)	2.056(5)	Ru(1)–N(6)	2.049(5)
N(1)–Ru(1)–N(2)	78.7(2)	N(1)–Ru(1)–N(3)	93.7(2)
N(1)–Ru(1)–N(4)	170.1(2)	N(1)–Ru(1)–N(5)	92.0(2)
N(1)–Ru(1)–N(6)	99.4(2)	N(2)–Ru(1)–N(3)	84.9(2)
N(2)–Ru(1)–N(4)	94.1(2)	N(2)–Ru(1)–N(5)	97.7(2)
N(2)–Ru(1)–N(6)	176.7(2)	N(3)–Ru(1)–N(4)	78.7(2)
N(3)–Ru(1)–N(5)	174.1(2)	N(3)–Ru(1)–N(6)	97.9(2)
N(4)–Ru(1)–N(5)	95.7(2)	N(4)–Ru(1)–N(6)	88.1(2)
N(5)–Ru(1)–N(6)	79.7(2)		

distorted octahedron with a bite angle of 79.0° averaged over three bidentate ligands. The mean Ru–N bond length for the complex (2.055 Å) is comparable with that published for $[\text{Ru}(\text{bpy})_3]^{2+}$ (2.053–2.056 Å) [26].

3.2. Viscosity studies

The measurement of DNA viscosity is regarded as the least ambiguous and the most critical test of a DNA binding model in solution in the absence of crystallographic structural data [27, 28]. A classical intercalation model usually results in lengthening the DNA helix as base pairs are separated to accommodate the bound ligand, which leads to an increase in DNA viscosity. In contrast, semi-intercalation of a ligand could bend or kink the DNA helix. The introduced bends or kinks in DNA would reduce its effective length and concomitantly, reduce its viscosity. Certain complexes, such as $[\text{Ru}(\text{bpy})_3]^{2+}$, which interact with DNA in an electrostatic binding mode, have no influence on DNA viscosity [29].

The changes in relative viscosity of rod-like CT-DNA in the presence of **1**, **2**, EB and $[\text{Ru}(\text{bpy})_3]^{2+}$ are shown in figure 2. EB has been well known to bind with DNA through intercalation, while $[\text{Ru}(\text{bpy})_3]^{2+}$ is known to bind with DNA in electrostatic mode, exerting essentially no effect on DNA viscosity. As can be seen in figure 2, the viscosity of DNA remains almost unchanged upon addition of either **1** or **2**. The viscosity exhibited by **1** or **2**

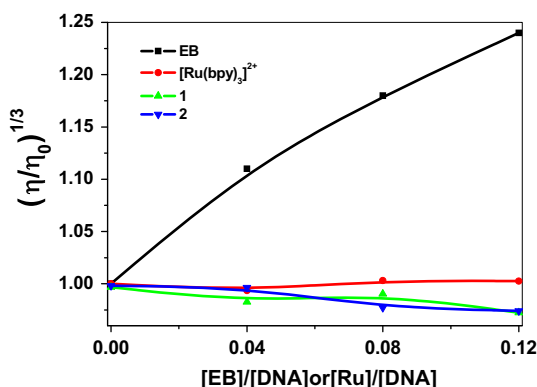


Figure 2. Effects of increasing amounts of **1** (▲), **2** (▼), EB (■), and $[\text{Ru}(\text{bpy})_3]^{2+}$ (●) on the relative viscosities of CT-DNA at 30.0 ± 0.1 °C, $[\text{DNA}] = 0.5$ mM, $r = [\text{Ru}]/[\text{DNA}]$.

bound to DNA was very similar to that of $[\text{Ru}(\text{bpy})_3]^{2+}$. The DNA viscosity experimental results suggest that **1** and **2** bind to DNA through an electrostatic binding mode.

3.3. Absorption spectra

Absorption spectra of **1** and **2** exhibit similar characteristics, *i.e.*, there are three bands with comparable intensity between 220 and 550 nm. The ultraviolet bands around 247 nm and 286 nm could be attributed to intraligand (IL) transition, and the visible band at 430 nm was assigned to metal-to-ligand charge transfer (MLCT) according to spectra of other Ru (II) complexes [30]. The electronic spectral traces of **1** and **2** with successive increase in CT-DNA at room temperature are given in figure 3. The absorption intensities of the three bands of the complexes successively decrease (as shown in figure 3 by the arrow symbols) upon addition of CT-DNA. The hypochromism ($H\%$) of MLCT bands in **1** and **2**, defined as $H\% = 100\% \cdot (A_{\text{free}} - A_{\text{bound}})/A_{\text{free}}$, was determined to be 9.85 and 8.64%, respectively.

To quantitatively compare the DNA-binding affinities of the two complexes, their intrinsic binding constants K_b to DNA were obtained from monitoring changes in the MLCT absorbance for both complexes according to equation (1) [31–35], where $[\text{DNA}]$ is the DNA concentration in nucleotides, ε_a is the extinction coefficient ($A_{\text{abs}}/[\text{M}]$) observed for the MLCT absorption band at a given DNA concentration, and ε_f and ε_b are, respectively, the extinction coefficients for the free Ru(II) complex and Ru(II) complex in the fully bound form. K_b is the equilibrium binding constant in M^{-1} , C_t is the total Ru(II) complex concentration, and s is the binding site size. Equation 1 (1a and 1b) is applied in absorption titration data to non-cooperative metallointercalators binding to CT-DNA.

$$(\varepsilon_a - \varepsilon_f)/(\varepsilon_b - \varepsilon_f) = (b - (b^2 - 2K_b^2 C_t [\text{DNA}]/s)^{1/2})/2K_b C_t \quad (1a)$$

$$b = 1 + K_b C_t + K_b [\text{DNA}]/2s \quad (1b)$$

From the decay of the absorbance, the intrinsic binding constants (table 3) K_b of **1** and **2** were determined to be $(5.7 \pm 0.3) \times 10^4 \text{ M}^{-1}$ and $(4.1 \pm 0.2) \times 10^4 \text{ M}^{-1}$, respectively. K_b of

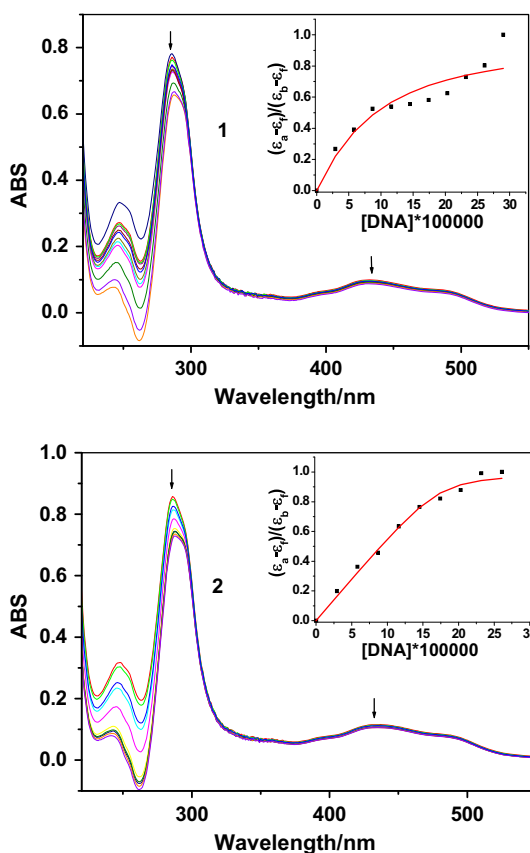


Figure 3. Absorption spectra of **1** and **2** in buffer A in the presence of increasing amounts of CT-DNA. [Ru] = 10 μM , [DNA] = 0–190 μM from top to bottom. Arrows indicate the change in absorbance upon increasing the DNA concentration. Inset: plot of $(\epsilon_a - \epsilon_f) / (\epsilon_b - \epsilon_f)$ versus [DNA] and the non-linear fit for the titration of DNA to Ru (II) complexes.

Table 3. Absorption spectra (λ_{max} /nm) and DNA-binding constants K_b ($\times 10^4 \text{ M}^{-1}$) of **1** and **2**.

Complex	λ_{max} (free)	λ_{max} (bound)	$\Delta\lambda$ (nm $^{-1}$)	H (%)	$K_b / (10^4 \text{ M}^{-1})$	s
1	431	432	1	9.85	5.7 ± 0.3	2.03 ± 0.37
	286	288	2	14.76		
	247	243	−4	71.80		
2	434	434	0	8.64	4.1 ± 0.2	0.86 ± 0.05
	286	288	2	15.01		
	248	242	−6	75.21		

1 is little greater than that of **2**, revealing a stronger DNA-binding affinity of **1**. Since the two complexes have similar structures, the difference comes mostly from the different dicationic ligands, where the methyl group in **1** gives less steric hindrance than the ethyl in **2**. The binding constants of both complexes are greater than that of $[\text{Ru}(\text{bpy})_3]^{2+}$ [36], suggesting that the charge increase in the ligands gives an affinity enhancement between the complexes and DNA.

3.4. Thermal denaturation studies

The thermal behavior of CT-DNA in the presence of complex can provide insight into their conformational changes with temperature and the interaction between the complexes and DNA. When the temperature in the solution increases, double-stranded DNA gradually dissociates to single strands and generates a hyperchromic effect on the absorption spectra of DNA bases ($\lambda_{\max} = 260$ nm). In order to identify this transition process, the melting temperature T_m , which is defined as the temperature where half of the total base pairs are unbonded, is usually introduced. As shown in figure 4, DNA melting experiments revealed that T_m of CT-DNA is 60.8 ± 0.2 °C in the absence of complexes. The observed melting temperature in the presence of **1** and **2** were 76.8 ± 0.4 °C and 74.1 ± 0.4 °C, respectively, at a concentration ratio $[\text{Ru}]/[\text{DNA}] = 1 : 10$. The obvious increases in T_m of the two complexes (the ΔT_m were 16.1 and 13.3 °C for **1** and **2**, table 4) indicate that both complexes can stabilize CT-DNA. This occurs because the synergistic effect on the positive charge in the ligand enhances the electrostatic interactions between the complex and the negatively charged phosphate backbone in DNA. The experimental results also indicate that **1** exhibits a larger DNA-binding affinity than **2**.

3.5. Enantioselective binding studies

Equilibrium dialysis experiments offer the opportunity to examine the enantioselectivity of complexes binding to DNA [37]. According to the proposed binding model by Barton [38], the Δ -enantiomer of the complex which is a right-handed propeller-like structure, displays greater affinity than the Λ -enantiomer with the right-handed CT-DNA helix. The greater affinity for right handed CT-DNA helix exhibited by the Δ -enantiomer of the complex can be attributed to more appropriate steric matching. Racemic solutions of the two complexes were dialyzed against CT-DNA for 12 h and then subjected to circular-dichroism (CD) analysis. As shown in figure 5, both of the dialysates of the Ru(II) complexes show strong CD signals with a positive (276 nm) and a negative band (297 nm). Complex **1** exhibits a stronger CD signal than **2**. Although neither of the complexes is resolved into pure enantiomers, both of the complexes show enantioselectivity when binding with DNA.

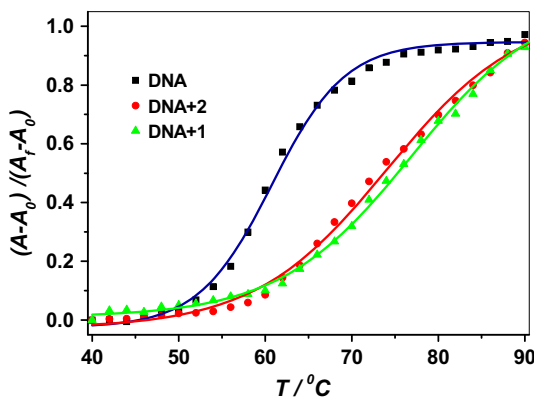
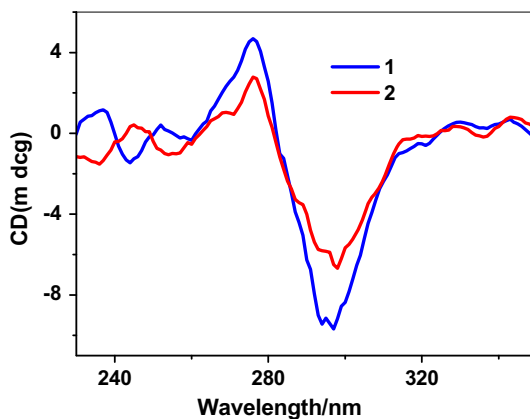


Figure 4. Normalized UV melting curves of CT-DNA in the absence (■) or presence of **1** (▲) and **2** (●), $[\text{DNA}] = 100$ μM , $r = [\text{Ru}]/[\text{DNA}]$.

Table 4. The effect of **1** and **2** on the T_m of CT-DNA ($r = [\text{Ru}] / [\text{DNA}] = 1:10$).

Complex	T_m (°C)	ΔT_m (°C)
CT-DNA	60.8 ± 0.2	
1 + CT-DNA	76.9 ± 0.4	16.12
2 + CT-DNA	74.1 ± 0.4	13.33

Figure 5. CD spectra of **1** and **2** in buffer A in the presence of CT-DNA, $[\text{Ru}] = 50 \mu\text{M}$, $[\text{DNA}] = 1.0 \text{ mM}$.

3.6. Photocleavage of pBR 322 DNA by Ru(II) complexes

The cleavage of plasmid DNA can be monitored by agarose gel electrophoresis. When circular plasmid DNA is subjected to electrophoresis, relatively fast migration will be observed for the intact supercoiled form (form I). If scission occurs on one strand (nicking), the supercoil will relax to generate a slower-moving open circular form (form II). If both strands are cleaved, a linear form (form III) that migrates between forms I and II will be generated [39]. Figure 6 shows gel electrophoresis separation of pBR322 DNA after incubation with **1** or **2** and irradiation at 365 nm. Only a slight amount of DNA cleavage is observed in the control where there is no metal complex (lane 0).

Approximately half of the supercoiled plasmid was converted to nicked form when 60 μM of **1** was used in photocleavage reactions (lane 3). Eighty micromole of **1** (lane 4) promoted the complete conversion of supercoiled DNA from Form I to Form II. However,

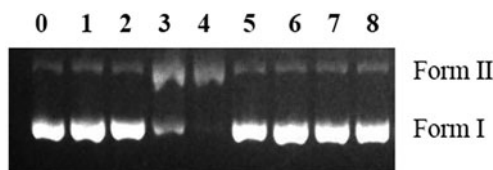
Figure 6. Photocleavage of supercoiled pBR322 DNA in the presence of **1** (lanes 1–4) and **2** (lanes 5–8) in 20, 40, 60, and 80 μM , respectively. All lanes are under irradiation at 365 nm for 60 min.

Table 5. The IC₅₀ (uM) values determined by MTT assay for the two ruthenium(II) complexes against different tumor cell lines.^a

Complex	A549	Hela	CNE-2
1	267 ± 30	452 ± 22	369 ± 21
2	246 ± 16	419 ± 17	234 ± 15
Cisplatin	11 ± 2	14 ± 3	8 ± 3

^aCells were treated with various concentrations of tested compounds for 48 h. IC₅₀ values were calculated as described in Section 2. Each value represents the mean ± SD of three independent experiments.

when **2** was used in photocleavage reactions, there was almost no DNA converted to nicked form. The difference in DNA-cleavage ability may originate from the different DNA-binding affinities of **1** and **2**.

3.7. Cytotoxicity assay

The *in vitro* antitumor potencies of the Ru(II) complexes (at concentrations from 6.25 to 400 μM) were determined against three tumor cell lines (cervical cancer (HeLa), human lung adenocarcinoma (A549), and human low differentiation nasopharyngeal carcinoma (CNE-2)) using the MTT assay. Complexes **1** and **2** were dissolved in DMSO and blank samples containing the same amount of DMSO were used as controls. Cisplatin was included as the positive control. Cisplatin demonstrated high levels of cytotoxicity against all cell lines, in accord with previous reports [13, 40]. Table 5 demonstrates the IC₅₀ values obtained from non-linear regression analysis of dose response data for the compounds tested. Both complexes demonstrate lower *in vitro* cytotoxicity than cisplatin against selected tumor cell lines. The two complexes displayed non-selective cytotoxic activity against all tumor cells tested. Complex **2** was more active against all the selected tumor cells than **1**, which is opposite to their order of DNA binding and ability to cleave DNA cleavage. Binding of **1** and **2** to biological targets other than DNA could be responsible for the observed cytotoxicity of the complexes. The same results were also found using two Zn complexes [41].

4. Conclusion

Two new Ru(II) complexes [Ru(bpy)₂(L)]⁴⁺ where the ligand L contains dicationic pendants have been synthesized. The results show that bpy with ammonium groups can cause some interesting differences in the properties of the resulting complexes. Both of the complexes bind to DNA by electrostatic binding mode. Complex **1** has a higher DNA affinity and DNA cleavage ability than **2**. Both complexes reveal good enantioselectivity when binding with CT-DNA. It is interesting to note, however, that **1** showed lower cytotoxicity than **2** against three human tumor cell lines. Therefore, biological targets other than DNA may be responsible for the *in vitro* cytotoxicity of the two Ru(II) polypyridine complexes.

Supplementary material

CCDC 928326 contains the supplementary crystallographic data for **1**. The data can be obtained free of charge via <http://www.ccdc.cam.ac.uk/conts/retrieving.html>, or from the Cambridge Crystallographic Data Center, 12 Union Road, Cambridge CB2 1EZ, UK; Fax: +44 1223 336 033; or Email: deposit@ccdc.cam.ac.uk.

Funding

We are grateful to the National Natural Science Foundation of China [grant number 21101034], Yong Teachers Training Plan of Guangdong Province [grant number Yq2013086], Science and Technology Plan of Dongguan City [grant number 2011108102046], and innovative item of undergraduate of Guangdong Province [grant number 1057112037].

Supplemental data

Supplemental data for this article can be accessed here [<http://dx.doi.org/10.1080/00958972.2014.977270>].

References

- [1] K.E. Erkkila, D.T. Odom, J.K. Barton. *Chem. Rev.*, **99**, 2777 (1999).
- [2] L.N. Ji, X.H. Zou, J.G. Liu. *Coord. Chem. Rev.*, **216–217**, 513 (2001).
- [3] J.G. Vos, J.M. Kelly. *Dalton Trans.*, **35**, 4869 (2006).
- [4] J.A. Thomas. *Chem. Soc. Rev.*, **36**, 856 (2007).
- [5] V. Pierroz, T. Joshi, A. Leonidova, C. Mari, J. Schur, I. Ott, L. Spiccia, S. Ferrari, G. Gasser. *J. Am. Chem. Soc.*, **134**, 20376 (2012).
- [6] G. Sava, A. Bergamo, S. Zorzet, B. Gava, C. Casarsa, M. Cocchietto, A. Furlani, V. Scarcia, B. Serli, E. Iengo, E. Alessio, G. Mestroni. *Eur. J. Cancer*, **38**, 427 (2002).
- [7] X.H. Zou, B.H. Ye, H. Li, Q.L. Zhang, H. Chao, J.G. Liu, L.N. Ji, X.Y. Li. *J. Biol. Inorg. Chem.*, **6**, 143 (2001).
- [8] P. Waywell, V. Gonzalez, M.R. Gill, H. Adams, A.J.H.M. Meijer, M.P. Williamson, J.A. Thomas. *Chem. Eur. J.*, **16**, 2407 (2010).
- [9] N.P. Cook, K. Kilpatrick, L. Segatori, A.A. Martí. *J. Am. Chem. Soc.*, **134**, 20776 (2012).
- [10] S.A. Poteet, M.B. Majewski, Z.S. Breitbach, C.A. Griffith, S. Singh, D.W. Armstrong, M.O. Wolf, F.M. MacDonnell. *J. Am. Chem. Soc.*, **135**, 2419 (2013).
- [11] M.R. Gill, J.A. Thomas. *Chem. Soc. Rev.*, **41**, 3179 (2012).
- [12] H. Paul, T. Mukherjee, M. Mukherjee, T.K. Mondal, A. Moirangthem, A. Basu, E. Zangrando, P. Chattopadhyay. *J. Coord. Chem.*, **66**, 2747 (2013).
- [13] Y.C. Wang, C. Qian, Z.L. Peng, X.J. Hou, L.L. Wang, H. Chao, L.N. Ji. *J. Inorg. Biochem.*, **130**, 15 (2014).
- [14] G.B. Jiang, J.H. Yao, G.J. Lin, H.L. Huang, X.Z. Wang, Y.J. Liu. *J. Coord. Chem.*, **66**, 2423 (2013).
- [15] E. Wachter, D.K. Heidary, B.S. Howerton, S. Parkin, E.C. Glazer. *Chem. Commun.*, **48**, 9649 (2012).
- [16] A. Arora, C. Balasubramanian, N. Kumar, S. Agrawal, R.P. Ojha, S. Maiti. *FEBS Journal.*, **275**, 3971 (2008).
- [17] J.K. Barton, A.T. Danishefsky, J. Goldberg. *J. Am. Chem. Soc.*, **106**, 2172 (1984).
- [18] J. Marmur. *J. Mol. Biol.*, **3**, 208 (1961).
- [19] J.H. Li, J.T. Wang, P. Hu, L.Y. Zhang, Z.N. Chen, Z.W. Mao, L.N. Ji. *Polyhedron*, **27**, 1898 (2008).
- [20] Y. An, Y.Y. Lin, H. Wang, H.Z. Sun, M.L. Tong, L.N. Ji, Z.W. Mao. *Dalton Trans.*, **35**, 2066 (2006).
- [21] J.P. Collin, J.P. Sauvage. *Inorg. Chem.*, **25**, 135 (1986).
- [22] G.M. Sheldrick, *SADABS 2.05*, University of Gottingen, Germany (1996).
- [23] G.M. Sheldrick. *SHELXS97 and SHELXL97.*, University of Gottingen, Germany (1996).
- [24] J.B. Chaires, N. Dattagupta, D.M. Crothers. *Biochemistry*, **21**, 3933 (1982).
- [25] G. Cohen, H. Eisenberg. *Biopolymers*, **8**, 45 (1969).
- [26] E.E. Pérez-Cordero, C. Campana, L. Echeleyen. *Angew. Chem. Int. Ed. Engl.*, **36**, 137 (1997).
- [27] S. Satyanarayana, J.C. Dabrowiak, J.B. Chaires. *Biochemistry*, **31**, 9319 (1992).
- [28] C.V. Kumar, J.K. Barton, N.J. Turro. *J. Am. Chem. Soc.*, **107**, 5518 (1985).
- [29] J.G. Liu, B.H. Ye, H. Li, Q.X. Zhen, L.N. Ji, Y.H. Fu. *J. Inorg. Biochem.*, **76**, 265 (1999).

- [30] J. Sun, S. Wu, Y. An, J. Liu, F. Gao, L.N. Ji, Z.W. Mao. *Polyhedron*, **27**, 2845 (2008).
- [31] R.B. Nair, E.S. Teng, S.L. Kirkland, C.J. Murphy. *Inorg. Chem.*, **37**, 139 (1998).
- [32] L.M. Chen, J. Liu, J.C. Chen, C.P. Tan, S. Shi, K.C. Zheng, L.N. Ji. *J. Inorg. Biochem.*, **102**, 330 (2008).
- [33] M.T. Carter, M. Rodriguez, A.J. Bard. *J. Am. Chem. Soc.*, **111**, 8901 (1989).
- [34] P. Uma Maheswari, M. Palaniandavar. *J. Inorg. Biochem.*, **98**, 219 (2004).
- [35] S. Shi, X.T. Geng, J. Zhao, T.M. Yao, C.R. Wang, D.J. Yang, L.F. Zheng, L.N. Ji. *Biochimie*, **92**, 370 (2010).
- [36] G. Yang, J.Z. Wu, L. Wang, L.N. Ji, X. Tian. *J. Inorg. Biochem.*, **66**, 141 (1997).
- [37] X. Meng, M.L. Leyva, M. Jenny, I. Gross, S. Benosman, B. Fricker, S. Harlepp, P. Hebraud, A. Boos, P. Wlosik, P. Bischoff, C. Sirlin, M. Pfeffer, J.-P. Loeffler, C. Gaididon. *Cancer Res.*, **69**, 5458 (2009).
- [38] J.K. Barton. *Science*, **233**, 727 (1986).
- [39] J.K. Barton, A.L. Raphael. *J. Am. Chem. Soc.*, **106**, 2466 (1984).
- [40] Y.C. Liu, Z.F. Chen, L.M. Liu, Y. Peng, X. Hong, B. Yang, H.G. Liu, H. Liang, C. Orvig. *Dalton Trans.*, **38**, 10813 (2009).
- [41] Q. Jiang, J.H. Zhu, Y.M. Zhang, N. Xiao, Z.J. Guo. *BioMetals*, **22**, 297 (2009).